Enhancement of fluorescence in inorganic dyes by metallic nanostructured surfaces

Kitsakorn Locharoenrat and Pattareeya Damrongsak

Department of Physics, Faculty of Science, King Mongkut's Institute of Technology Ladkrabang, Bangkok 10520, Thailand, kitsakorn.lo@kmitl.ac.th

Received: 13.11.2015

Abstract. We have studied the influence of shape and chemical content of metallic nanostructures (gold-palladium core–shell nanorods, gold nanobipyramids and single-crystalline porous palladium nanocrystals) on the luminescence of Rhodamine 6G and Coumarin153 dyes. The changes found in the emission intensity are attributed to different proportions of the dyes and the metallic nanostructures. The enhancement of the fluorescence observed by us for the cases of Rhodamine 6G with gold-palladium core–shell nanorods and Rhodamine 6G with gold nanobipyramids suggests their promising plasmonic properties. This may be regarded as a preliminary step towards development of the fluorescent probes possessing high photo-sensitivity.

Keywords: metals, gold, nanostructures, palladium, plasmonic resonance

PACS: 33.50.Dq, 78.67.Qa, 78.67.Rb
UDC: 535.33

1. Introduction

Plasmonic-resonance properties of metallic nanoparticles have been extensively used to tailor the optical properties of organic molecules. Interactions of these nanoparticles with organic-dye molecules can become a basis for many applications, e.g. nanoscale lasers [1], surface-enhanced Raman spectroscopy [2–3] and plasmon-enhanced fluorescence spectroscopy [4]. These interactions can also play a key role in the photonic nanodevices. Metallic nanoparticles are able to either quench or enhance the intrinsic luminescence of an emitter, depending on the distance between the donor and the emitter. In general, when the incident light falls onto a surface of metallic nanoparticles, the enhancement of the fluorescence comes from the surface plasmon resonance. This plasmonic property results in increasing excitation decay rate and increasing radiative quantum efficiency. Moreover, the dipole energy accumulated at the surface of metallic nanoparticles can suppress the ratio of the radiative to non-radiative decay rates through the energy-transfer mechanism, thus leading to quenching of the intrinsic fluorescence from the dye molecules [5].

Up to date, a number of studies have been reported on the properties of combinations of metallic nanoparticles with dyes. They have demonstrated that the metallic nanoparticles can affect the emission intensity of the dyes. Nonetheless, these works have mainly studied the effect of size and concentration of the nanoparticles. Although various shapes of metallic nanostructures have been dealt with in the past decade [6–8], the results concerned with introduction of the metallic nanoparticles into fluorescent materials are still limited. This implies a necessity for the further researches in this direction.

In this work we focus on the effect of plasmonic interactions occurring in the metallic nanostructures of different shapes, namely gold-palladium core–shell nanorods (abbreviated

further on as Au@Pd NRs), gold nanobipyramids (Au NBPs) and porous single-crystalline Pd nanocrystals (Pd PNCs), on the fluorescence of Rhodamine 6G (Rh6G) and Coumarin153 (C153) dyes. These dyes have been chosen because they are well enough studied and manifest good photostability and high quantum yields [9, 10]. In addition, they are widely used as fluorescent probes in various fields, e.g. in biology, chemistry and medicine (see Refs. [11–13]). For photovoltaic applications, one can use the enhancement of fluorescence in these dyes, which takes place in thin solid films.

2. Experimental

2.1. Samples

Rhodamine 6G and Coumarin153 were obtained from Aldrich, USA. Au@Pd NRs, Au NBPs and Pd PNCs were purchased from Nanoseedz Ltd, Hong Kong. These metallic nanostructures were studied with respect to their influence on the fluorescence emission of the dyes. The main idea behind our choice was overlapping of the absorption spectra of these nanostructures with the fluorescent spectra of the dyes, as illustrated in Fig. 1. In our experiments, three sets of solutions referred to as A, B and C were prepared (see Tables 1 to 3).

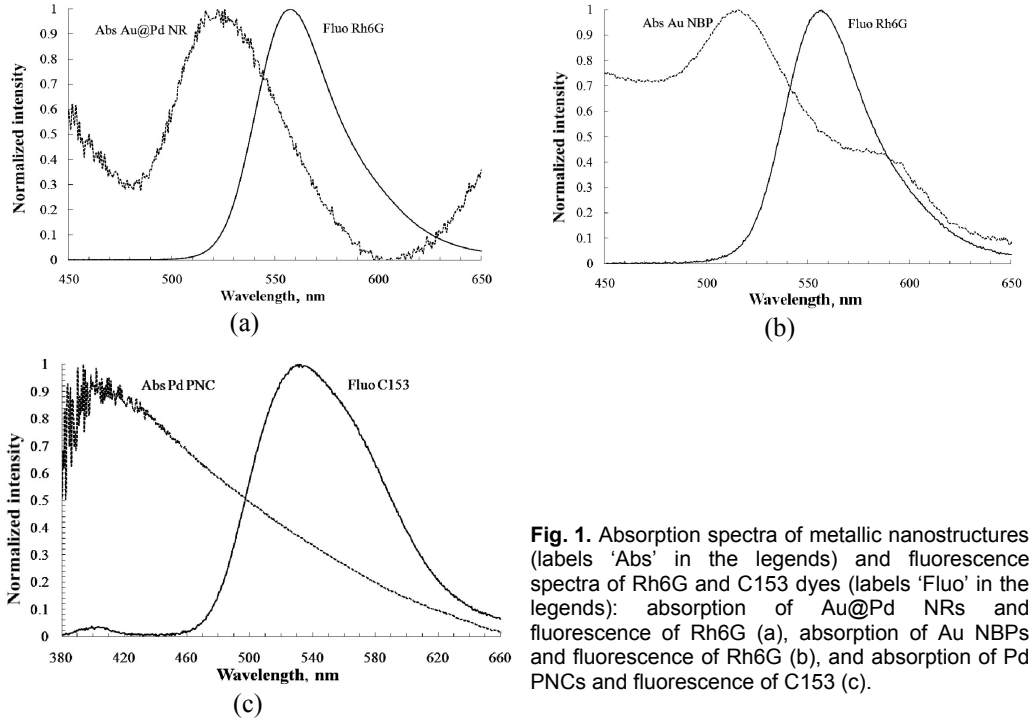

Fig. 1. Absorption spectra of metallic nanostructures (labels 'Abs' in the legends) and fluorescence spectra of Rh6G and C153 dyes (labels 'Fluo' in the legends): absorption of Au@Pd NRs and fluorescence of Rh6G (a), absorption of Au NBPs and fluorescence of Rh6G (b), and absorption of Pd PNCs and fluorescence of C153 (c).

Table 1. Description of set A of metallic-nanostructure solutions in dyes.

Sample	Reference (Rh6G in deionized water) M *	Sample (Rh6G + Au@Pd NRs)	
		Rh6G (M)	Au@Pd (M)
A1	1.50×10^{-6}	1.50×10^{-6}	3.05×10^{-3}
A2	7.50×10^{-7}	7.50×10^{-7}	$15.25\text{x}10^{-4}$
A3	3.75×10^{-7}	3.75×10^{-7}	$76.25\text{x}10^{-5}$
A4	$1.88\text{x}10^{-7}$	$1.88\text{x}10^{-7}$	38.12×10^{-5}
A5	9.38×10^{-8}	9.38×10^{-8}	19.06×10^{-5}

* 'M' means 'molar'

Table 2. Description of set B of metallic-nanostructure solutions in dyes.

Sample	Reference (Rh6G in deionized water) M *	Sample (Rh6G + Au NBPs)	
		Rh6G (M)	Au (M)
B1	1.00×10^{-6}	1.00×10^{-6}	83.8×10^{-3}
B2	0.50×10^{-6}	0.50×10^{-6}	41.9×10^{-3}
B3	2.50×10^{-7}	$2.50\text{x}10^{-7}$	20.9×10^{-3}
B4	1.25×10^{-7}	1.25×10^{-7}	10.5×10^{-3}
B5	6.25×10^{-8}	6.25×10^{-8}	5.24×10^{-3}

* 'M' means 'molar'

Table 3. Description of set C of metallic-nanostructure solutions in dyes.

Sample	Reference (C153 in ethanol) M*	Sample (C153 + Pd PNCs)	
		Cou153 (M)	Pd (M)
C1	270.83×10^{-8}	270.83×10^{-8}	14.68×10^{-3}
C2	268.75×10^{-8}	268.75×10^{-8}	7.34×10^{-3}
C3	267.70×10^{-8}	267.70×10^{-8}	3.67×10^{-3}
C4	267.19×10^{-8}	267.19×10^{-8}	$1.83\text{x}10^{-3}$
C5	266.92×10^{-8}	266.92×10^{-8}	0.91×10^{-3}

* 'M' means 'molar'

2.2. Experimental section

The absorption spectra of our samples prepared as explained above were measured in the wavelength region 350–800 nm, using an optical spectrometer Avantes 2048. A tungsten lamp was used as a light source. To measure the fluorescence spectra of the dyes, high-power green light emitting diodes (the excitation wavelength 516 nm and the power 1 W) were used for exciting Rh6G and ultraviolet light emitting diodes (the excitation wavelength 398 nm and the power 1 W) for exciting C153. A right-angle detection scheme was employed, as shown in Fig. 2.

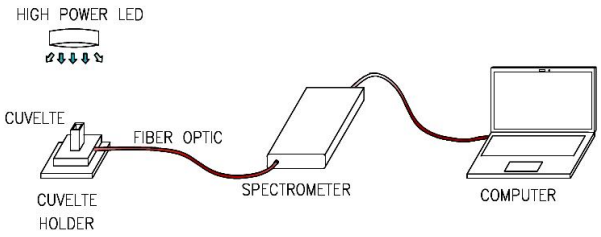

Fig. 2. Schematic diagram of measurements of the fluorescence spectra based upon right-angle detection geometry.

3. Results and discussion

Fig. 3 illustrates only some of many examples of the detailed fluorescence spectra for the dyes obtained in the presence (or absence) of the metallic nanostructures, Au@Pd NRs, Au NBPs and Pd PNCs, which have different shapes.

As seen from Fig. 3, the fluorescence signal from the dyes can be enhanced by adding the metallic nanostructures. This is accompanied by virtually no changes in the spectral shapes. The exception is the system denoted in concise form as Rh6G + Au@Pd NRs, for which the spectral shape becomes somewhat different from that of the pure dye. Namely, the spectral maximum of the fluorescence intensity for the latter system reveals a clear blue shift. Perhaps, the reason lies in

collisions of Rh6G with Au@Pd NRs, which can change the local dielectric environment of the nanorods. The enhancement of the emission observed by us is explained by the two reasons. The first is an increased absorption rate of the dyes due to plasmonic coupling with the metallic nanostructures. The second is a possibility of orientation of the metallic nanostructures, which controls the plasmonic interactions between the metallic nanostructures and the dye molecules.

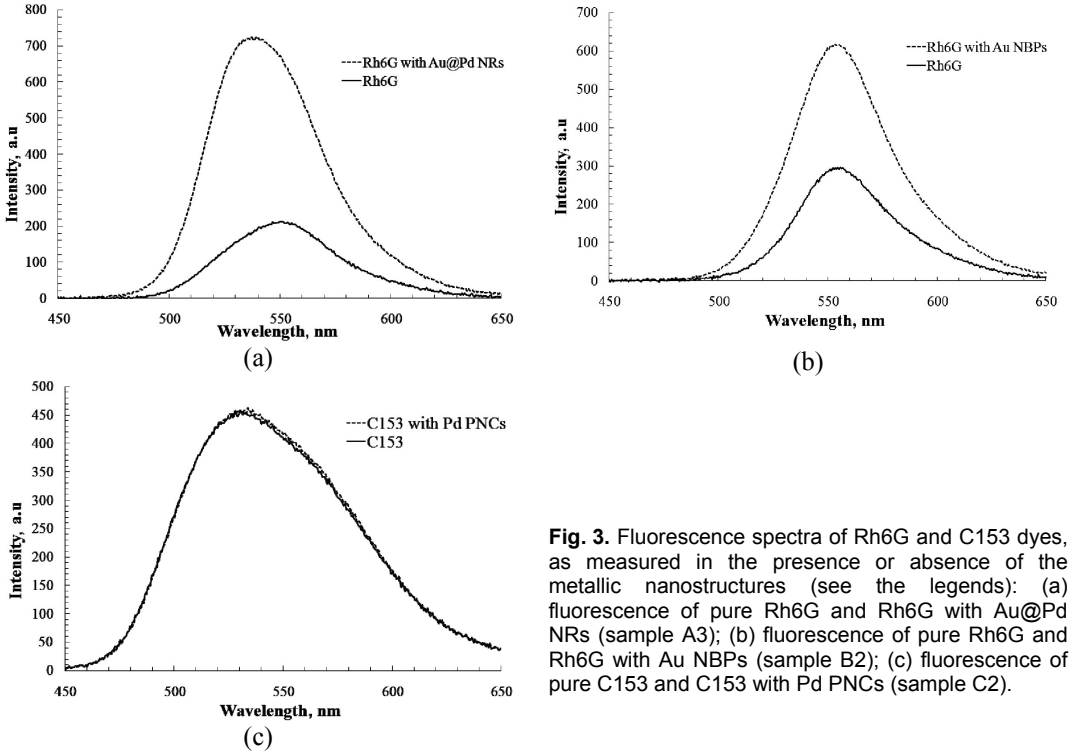

Fig. 3. Fluorescence spectra of Rh6G and C153 dyes, as measured in the presence or absence of the metallic nanostructures (see the legends): (a) fluorescence of pure Rh6G and Rh6G with Au@Pd NRs (sample A3); (b) fluorescence of pure Rh6G and Rh6G with Au NBPs (sample B2); (c) fluorescence of pure C153 and C153 with Pd PNCs (sample C2).

In order to examine quantitatively the influence of concentration of the metallic nanostructures on the emission intensities measured for our dyes, we have calculated the ratio of the peak fluorescence intensity for the dye–nanoparticles mixture and the relevant peak intensity for the pure dye. The values of this parameter obtained for different samples under test are displayed in Fig. 4.

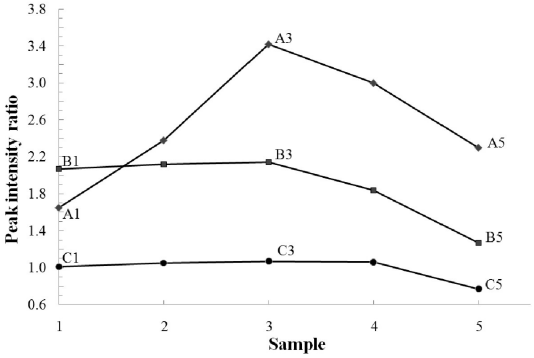

Fig. 4. Enhancement of peak fluorescence intensities for the dyes Rh6G or C153 calculated for the sample sets A, B and C.

The dye molecules are located very close to the metallic nanostructures at high concentrations of the metals and the dyes (e.g., for the samples A1, B1 and C1). Then the non-

radiative transfer of charge carriers to the metallic nanostructures could also be significant, thus leading to decreasing fluorescence intensity. The fluorescence intensity becomes higher when the metal and dye concentrations decrease (e.g., for the samples A2, B2 and C2). This seems to be natural because the spacing between the dye molecules and the nanostructures increases and only a small number of dye molecules can couple with the metallic nanostructures. Another reason comes from weakening of the non-radiative transfer mechanism.

There exists an optimum concentration that provides efficient plasmonic interactions for each set of our samples (e.g., for the cases referred to as A3, B3 and C3). Under these optimum conditions, the fluorescence intensity is enhanced approximately by 3.5 times for the system Rh6G + Au@Pd NRs, by 2.2 times for Rh6G + Au NBPs, and by 1.1 times for C153 + Pd PNCs. Beyond this optimum (see, e.g., the data for the samples A5, B5 and C5), the fluorescence intensity tends to decrease again with decreasing concentrations of the dye–nanoparticles mixtures. Probably, this can arise from re-quenching of the intrinsic fluorescence originated from mis-matched concentrations of the solutions. This finding should be further confirmed by the theo-retical calculations based upon the finite-difference time-domain technique. The latter will be a subject of our forthcoming study.

4. Conclusion

In the present work, we have investigated potential enhancement of the fluorescence emission of the standard dyes Rhodamine 6G and Coumarin153 doped with the metallic nanostructures of three different shapes. These are gold-palladium core–shell nanorods, gold nanobipyramids, and single-crystalline porous palladium nanocrystals. We have obtained the *highest* (more than threefold) fluorescence *enhancement* on the system of Rhodamine 6G mixed with the gold-palladium core–shell nanorods. On the contrary, the smallest fluorescence changes have been observed for Coumarin153 that involves the porous single-crystalline palladium nanocrystals.

Acknowledgement

The authors thank Ms. Nichakorn Boonpiphobanun for helpful discussions.

References

1. Noginov M A, Zhu G, Belgrave A M, Bakker R, Shalaev V M, Narimanov E E, Stout S, Herz E, Suteewong T and Wiesner U, 2009. Demonstration of a spaser-based nanolaser. Nature. **460**: 1110–1112.
2. MacLaughlin C M, Mullaithilaga N, Yang G, Ip S Y, Wang C and Walker G C, 2013. Surface-enhanced Raman scattering dye-labeled Au nanoparticles for triplexed detection of Leukemia and Lymphoma cells and SERS flow cytometry. Langmuir. **29**: 1908–1919.
3. Lim D K, Jeon K S, Hwang J H, Kim H, Kwon S, Suh Y D and Nam J M, 2011. Highly uniform and reproducible surface-enhanced Raman scattering from DNA-tailorable nanoparticles with 1-nm interior gap. Nature Nanotechnol. **6**: 452–460.
4. Iosin M, Baldeck P and Astilean S, 2009. Plasmon-enhanced fluorescence of dye molecules. Nucl. Instrum. Meth. in Phys. Res. B. **267**: 403–405.
5. Kang K A, Wang J, Jasinski J B and Achilefu S, 2011. Fluorescence manipulation by gold nanoparticles: From complete quenching to extensive enhancement. J. Nanobiotechnol. **9**: 16.
6. Lee J H, Gibson K J, Chen G and Weizmann Y, 2015. Bipyramid-templated synthesis of monodisperse anisotropic gold nanocrystals. Nature Commun. **6**: 7571.

7. Henning A M, Watt J, Miedziak P J, Cheong S, Santonastaso M, Song M, Takeda Y, Kirkl A I, Taylor S H and Tilley R D, 2013. Gold–palladium core–shell nanocrystals with size and shape control optimized for catalytic performance. Ang. Chemie. **52**: 1477–1480.
8. Zhnag J, Feng C, Deng Y, Liu L, Wu Y, Shen B, Zhong C and Hu W, 2014. Shape-controlled synthesis of palladium single-crystalline nanoparticles: The effect of HCl oxidative etching and facet-dependent catalytic properties. Chem. Mater. **26**: 1213–1218.
9. Kubin R F and Flethcher A N, 1982. Fluorescence quantum yields of some rhodamine dyes. J. Lumin. **27**: 455–462.
10. Li H, Cai L and Chen Z. Advances in chemical sensors. New York: InTech (2012).
11. So H S, Rao B A, Hwang J, Yesudas K and Son Y A, 2014. Synthesis of novel squaraine–bis(rhodamine-6G): A fluorescent chemosensor for the selective detection of Hg^{2+}. Sensors and Actuators B: Chemical. **202**: 779–787.
12. Zhang L, Wang J, Fan J, Guo K and Peng X, 2011. A highly selective, fluorescent chemosensor for bioimaging of Fe^{3+}. Bioorganic and Medicinal Chem. Lett. **21**: 5413–5416.
13. Wagner B D, 2009. The use of Coumarins as environmentally-sensitive fluorescent probes of heterogeneous inclusion systems. Molecules. **14**: 210–237.

Kitsakorn Locharoenrat and Pattareeya Damrongsak. 2016. Enhancement of fluorescence in inorganic dyes by metallic nanostructured surfaces. Ukr.J.Phys.Opt. **17**: 21 – 26.

Анотація. *У роботі вивчено вплив форми металічних наноструктур (золото-паладієвих наностержнів, золотих нанобіпірамід і монокристалічних пористих нанокристалів паладію) на поведінку флюоресценції люмінесцентних барвників – родаміну 6G і кумарину 153. Зміни інтенсивності випромінювання пов'язані зі співвідношенням вмісту барвників і металічних наноструктур. Виявлене нами підсилення флюоресценції родаміну 6G із золото-паладієвими наностержнями і золотими нанобіпірамідами перспективне з точки зору плазмонних властивостей. Воно є попереднім кроком у розвитку високофоточутливих флуоресцентних зондів.*